Science of the Total Environment 654 (2019) 895–905

Contents lists available at ScienceDirect

Science of the Total Environment

journal homepage: www.elsevier.com/locate/scitotenv

Footprints from the past: The influence of past human activities on vegetation and soil across five archaeological sites in Greenland

Rasmus Fenger-Nielsen [a,b], Jørgen Hollesen [a], Henning Matthiesen [a], Emil Alexander Sherman Andersen [c], Andreas Westergaard-Nielsen [b], Hans Harmsen [d], Anders Michelsen [b,c], Bo Elberling [b,*]

[a] Department of Conservation and Natural Sciences, The National Museum of Denmark, IC Modewegsvej, Brede, DK-2800 Lyngby, Denmark
[b] Center for Permafrost (CENPERM), Department of Geosciences and Natural Resource Management, University of Copenhagen, Øster Voldgade 10, DK-1350 Copenhagen K. Denmark
[c] Terrestrial Ecology Section, Department of Biology, University of Copenhagen, Universitetsparken 15, DK-2100 Copenhagen, Denmark
[d] Greenland National Museum & Archives, Hans Egedesvej 8, Boks 145, 3900 Nuuk, Greenland

HIGHLIGHTS

- Arctic archaeological sites are 'hotspots' of vegetation and plant nutrients.
- Human activities are evident in the vegetation even centuries after abandonment.
- Vegetation on archaeological sites is markedly different from the natural environment.
- Distinct vegetation makes archaeological sites detectable through satellite imagery.

GRAPHICAL ABSTRACT

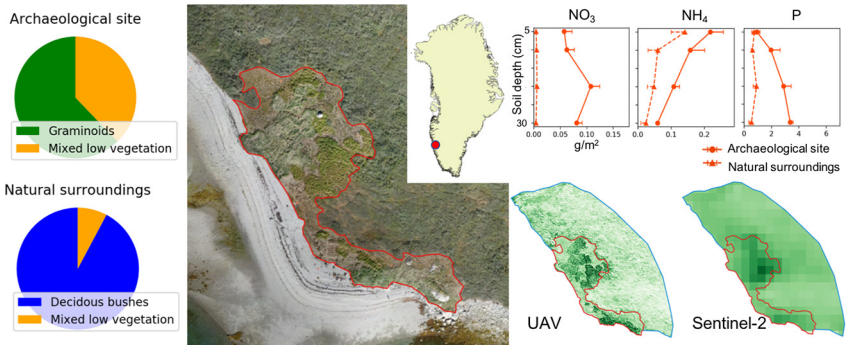

ARTICLE INFO

Article history:
Received 17 September 2018
Received in revised form 31 October 2018
Accepted 2 November 2018
Available online 8 November 2018

Editor: Elena PAOLETTI

Keywords:
Climate change
Arctic
Plant biomass
Soil chemistry
Archaeological remains
Remote sensing

ABSTRACT

Climate change has irrevocable consequences for the otherwise well-preserved archaeological deposits in the Arctic. Vegetation changes are expected to impact archaeological sites, but currently the effects are poorly understood. In this article we investigate five archaeological sites and the surrounding natural areas along a climate gradient in Southwest Greenland in terms of vegetation types, above- and below-ground biomass, soil geochemistry and spectral properties. The investigations are based on data from site-sampling and optical remote sensing from an unmanned aerial vehicle (UAV) and satellites. Results show that the archaeological sites are dominated by graminoids with approximately two times more above- and below-ground biomass than the surrounding areas, where the vegetation is more heterogeneous. This difference is associated with a 2–6 times higher content of plant available phosphorus and water extractable nitrate and ammonium in the archaeological deposits compared to the surrounding soil. Furthermore, the vegetation at archaeological sites is less affected by the regional climate variations than the surrounding natural areas. This suggests that soil-vegetation interactions at archaeological sites are markedly different from the natural environment. Thus, the long-term vulnerability of buried archaeological remains cannot be assessed based on existing projections of Arctic vegetation change. Finally, the study demonstrates that vegetation within archaeological sites has distinct spectral properties, and there is a great potential for using satellite imagery for large scale vegetation monitoring of archaeological sites and for archaeological prospection in the Arctic.

* Corresponding author at: Center for Permafrost (CENPERM), Department of Geosciences and Natural Resource Management, University of Copenhagen, Øster Voldgade 10, DK-1350 Copenhagen K, Denmark
E-mail address: be@ign.ku.dk (B. Elberling).

https://doi.org/10.1016/j.scitotenv.2018.11.018
0048-9697/

1. Introduction

Archaeological deposits in the Arctic are known for unique preservation of organic materials due to cold temperatures and often moist conditions (Elberling et al., 2011; Hollesen et al., 2016; Meldgaard, 2004; Rasmussen et al., 2010). These deposits contain animal bones, household waste and artefacts as well as paleoenvironmental proxies such as pollen and macrofossils (Grønnow, 1994; Meldgaard, 2004; Sandweiss and Kelley, 2012). In that way, the deposits provide an irreplaceable source of information for understanding past human behaviour and habitation in the Arctic.

Climate change has an enormous impact on the Arctic environment (IPCC, 2013), with irrevocable consequences for archaeological sites in the region (Hollesen et al., 2018). Critical well-known effects include physical destruction due to coastal erosion (Lantuit et al., 2012; O'Rourke, 2017) and increased microbial degradation of organic archaeological deposits as a result of warmer temperatures and a changing hydrology (Hollesen et al., 2016). In addition, climate change has promoted a well-documented 'greening' of the Arctic (Elmendorf et al., 2012; Epstein et al., 2012; Jia et al., 2003; Myers-Smith et al., 2015). These vegetation changes are expected to impact Arctic archaeological sites (Hollesen et al., 2018), but are still poorly understood and undescribed in an Arctic context.

Studies beyond the Arctic region have shown that vegetation cover may have a major impact on archaeological sites, with mostly negative consequences for preservation conditions (Crow and Moffat, 2005; Lisci et al., 2003; Tjelldén et al., 2015). These include direct effects, where plant roots penetrate and destroy archaeological objects or modify the stratigraphy of the deposits, which can directly lead to the loss of archaeological data (Tjelldén et al., 2015). Indirect effects include summer evapotranspiration that decreases soil moisture content (Swann et al., 2010). This process subsequently increases the oxygen supply, leading to accelerated microbial decomposition of organic archaeological deposits (Hollesen et al., 2016). At the same time, vegetation cover may have positive consequences for archaeological sites, stabilizing and protecting the soil against coastal, fluvial, and aeolian erosion (Gyssels et al., 2005; Wolfe and Nickling, 1993).

Arctic archaeological sites can often be recognized in the field based on a distinctly different and robust plant cover compared to surrounding areas. This observation is supported by a few studies in the Arctic, showing that archaeological sites are frequently dominated by graminoids and contain more plant biomass and nutrients than the surrounding natural environment (Derry et al., 1999; Forbes, 1996; Forbes et al., 2001). This is in contrast to Arctic ecosystem types in general, where plant growth is considered limited by low nutrient availability, in particular nitrogen and phosphorus (Elser et al., 2007; Schmidt et al., 1997).

In this study, we analysed vegetation and soil characteristics at five archaeological sites in the low-arctic region of the Nuuk fjord. The sites in our study area are located along a climate gradient stretching from the outer coast to the inner fjord and represent a suite of different climatic and environmental conditions. At each study site, we analyse vegetation, biomass, and soil nutrients in plots from the archaeological site and from the surrounding reference areas showing low to negligible visible impact from past human disturbance. We used an unmanned aerial vehicle (UAV) to map vegetation cover and measure the spectral properties of the archaeological sites and surrounding areas. The spectral properties are also investigated in a seasonal context based on multi-temporal satellite imagery (Sentinel-2). Finally, we compare the site-specific UAV imagery to optical satellite imagery of different spatial resolutions and discuss the potential for using satellite imagery for monitoring and discovering archaeological sites in the Arctic. The study represents a unique approach to comparing vegetation cover at archaeological sites at multiple different scales: hyper-local scale ground measurements through plot sampling, local scale through UAVs, and regional scale through satellite imagery to reveal spatial and temporal trends. The study is based on the underlying hypotheses: 1) vegetation cover (plant species composition and biomass) at archaeological sites is markedly different from the surrounding natural environment; 2) differences in vegetation cover between archaeological sites and reference areas are closely related to soil characteristics including plant available nitrogen and phosphorus; and 3) differences in vegetation cover is reflected in a spectral signal that makes it possible to distinguish archaeological sites from the surrounding natural environment using optical UAV and satellite imagery.

2. Materials and methods

2.1. Study sites

In August 2016 we investigated five archaeological sites in Southwest Greenland located in the Nuuk fjord (Fig. 1; Supplementary Table S1). This region is characterized by low arctic vegetation (Walker et al., 2005), and sporadic permafrost may occur. The five sites are located along a west-east transect and contain remains of the three main cultures of Greenland: Saqqaq (2500–800 BCE), Dorset (300 BCE–600 CE) and Thule/Historic Inuit (1300 CE–1900 CE), as well as Norse farmers inhabiting the Western Settlement (985 – ca. 1450 CE) (Supplementary Table S1). All sites are settlements with ruins and contain well-preserved organic archaeological materials. The sites represent contrasting conditions in terms of age, type of archaeological deposits and the different meteorological conditions found in the outer and inner fjord.

2.2. Site specific meteorological conditions

Monitoring equipment was installed at the five study sites to investigate variations in meteorological conditions. Measurements include air temperatures (Campbell Scientific 107 probes), soil temperatures at 10 cm depth (Campbell Scientific 107 probes), soil moisture content at 5 cm depth (Delta T, SM300) and precipitation (Campbell Scientific 52,202 tipping bucket rain gauge). Measurements were made at time intervals that ranged between 1 and 12 h from 1 September 2016 to 31 July 2017. Site-specific temperature measurements complement data sets from two official meteorological stations located in Nuuk and Kapisillit operated by Asiaq-Greenland Survey from 2000 to 2015 (Fig. 1). To investigate the variations in measured air temperatures between the study sites, we calculated the number of thawing degree days (TDD) and freezing degree days (FDD) according to Permafrost Subcommittee (1988).

2.3. Plot scale investigations

At each study site we did a paired sampling with six replicate plots (1×1 m) within the archaeological site and a further six replicate plots within a surrounding reference area. The archaeological plots were selected to represent the middens but to avoid areas influenced by excavations. The archaeological areas were defined by archaeologists from the Greenland National Museum based on site inspections and sub-surface testing. The reference plots were selected randomly in the surrounding area showing low to negligible visual impact from past human disturbance. Plots were within a maximum radius of 130 m away from the core area of the archaeological sites and areas with visible bedrock were avoided. Identifying the reference plots was a compromise between having environmental and topographical conditions similar to the archaeological sites (including slope, aspect, geology, wind, and wave exposure) and being outside the area directly impacted by past human activity. Maps of each study site with plot locations are presented in Supplementary Fig. S1. The plant species composition and plant cover percentage were investigated using the pin-point method and a 1×1 m frame with 25 fixed grid points. As the vegetation is multi-layered with a leaf area index >1, the total plant coverage (the

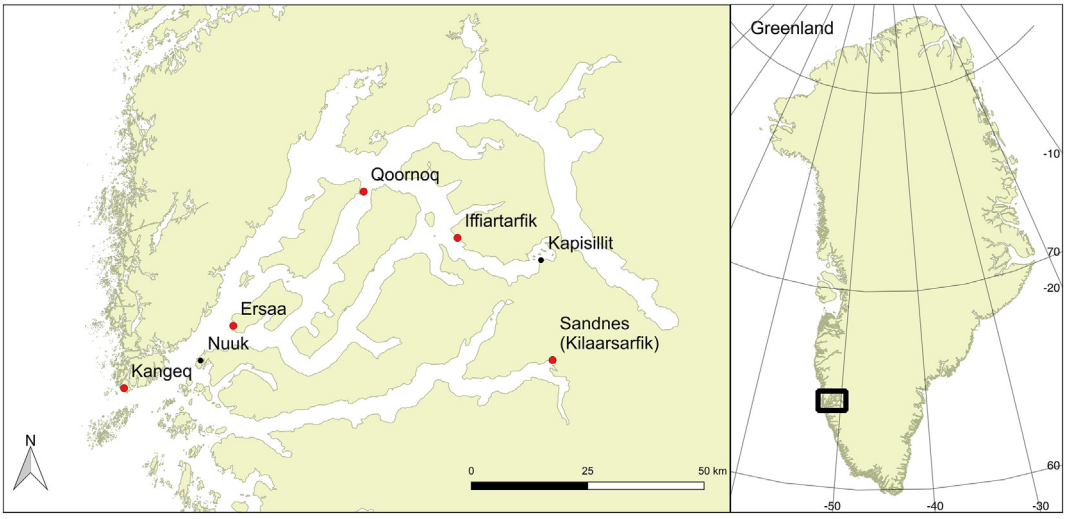

Fig. 1. The five study sites (red dots) are located in Southwest Greenland in the Nuuk region along a west-east transect stretching from the outer coast to the inner fjord.

sum of the coverage of the different plant species) may exceed 100%. After this, a sample of the living green biomass was collected from a sub-plot of 20 × 20 cm. Green plant parts were harvested at ground level and stored in paper bags for drying. Volume-specific soil samples (100 cm^3) were taken at 5, 10, 20 and 30 cm depths. The soil samples were packaged in zip-lock bags and frozen for transport to the analytical laboratory at the University of Copenhagen.

2.4. Laboratory analyses

The above-ground biomass samples were dried at room temperature and individually weighed. Each soil sample was sieved (2 mm) and plant roots were collected, dried, and weighed. The fraction of the soil finer than 2 mm was split into three sub-samples. From sub-sample one, water extractions were carried out using 5 g soil and 25 ml H_2O. The water extractions were analysed for ammonium (NH_4^+-N), nitrate (NO_3^--N) and total dissolved nitrogen (TDN) using a flow injection analyser (FIAstar 5000, Höganäs, Sweden). Based on NH_4^+, NO_3^-, and TDN measurements, dissolved organic nitrogen (DON) was calculated. Additionally, samples were analysed for dissolved organic carbon (DOC) on a Shimadzu TOC-5000A (Shimadzu, Kyoto, Japan). Sub-sample two was analysed for Olsen P, which is considered an estimate of plant available phosphorus (Delgado and Torrent, 1997; Olsen et al., 1954). Analyses were carried out by AGROLAB Agrar und Umwelt GmbH, Sarsted, Germany. From sub-sample three, pH was measured in aqueous suspension using 4 g soil and 10 ml H_2O. The remaining soil of sub-sample three was dried for 48 h at 80 °C, and the original water content calculated. The dried soil was ground and 10 mg samples segregated into tin combustion cups to measure total carbon and nitrogen contents and isotopic ratios of $^{13}C/^{12}C$ and $^{15}N/^{14}N$. This was obtained through Dumas combustion (1020 °C) on an elemental analyser (Flash 2000, Thermo Scientific, Bremen, Germany) coupled in continuous flow mode to a Thermo Delta V Advantage isotope ratio mass spectrometer. Acetanilide (Merck, Darmstadt, Germany) and soil standards (Elemental Microanalysis, Okehampton, UK) were used for elemental analyser mass calibration. As a working standard for isotope ratio analysis, we used pure gases of CO_2 and N_2 calibrated against certified reference materials of ^{13}C-sucrose and ^{15}N-$(NH_4)_2SO_4$, respectively (IAEA, Vienna, Austria). Performance of analysis was assessed by the inclusion of reference samples of biological origin (Peach leaves (NIST 1547), National Institute of Standards and Technology, Gaithersburg, MD, USA).

2.5. Remote sensing data

2.5.1. UAV investigations

All five sites were surveyed using a UAV equipped with a consumer-grade Red-Green-Blue (RGB) camera (Sony RX100iii) to compliment the plot scale investigations. In addition, a four-band (green, red, red-edge, near-infrared [NIR]) multispectral sensor (Parrot Sequoia) was employed at two sites (Iffiartafik and Kangeq). The data was collected using a Tarot 650 quadcopter and all surveys performed under stable light conditions at altitudes below 100 m above the ground. Six to ten ground control points (GCPs) were distributed and measured using a Trimble R8 RTK differential GPS (Trimble Inc., Sunnyvale, USA) for georeferencing resulting image mosaics. Additionally, five grey-scale reflectance targets were distributed, and the reflectance of each target was measured immediately before and after each flight with a spectroradiometer (ASD FieldSpec HH, Malvern Panalytical Ltd., UK). The raw multispectral images were converted to irradiance following the Parrot SEQ-AN-01 application note (Parrot, 2017). The irradiance images were then converted to surface reflectance using the information from the reflectance targets and the empirical line method (Smith and Milton, 1999). From both the RGB- and the multispectral images, orthomosaics were processed using Agisoft Photoscan 1.4 (Agisoft LLC, St. Petersburg, Russia). The resulting spatial resolution was 1.4–2.5 cm for the RGB mosaics and 7–8.2 cm for the multispectral mosaics. The spatial accuracy was <0.1 m for the RGB mosaics and < 0.5 m for the multispectral mosaics (see list of UAV-mosaics and further details in Supplementary Table S2). The RGB mosaics were used for mapping the vegetation cover at the site level. Multispectral mosaics were used to obtain additional information on the spectral reflectance of the vegetation cover and for comparison with coarser resolution satellite imagery.

2.5.2. Multi-temporal satellite imagery

Because the plot scale and UAV investigations only represent a snapshot in time, we included Sentinel-2 satellite imagery to observe spectral changes throughout the 2016 growing season. Sentinel-2 is a constellation of two satellites with a multispectral high-resolution sensor operated by the European Space Agency. The first satellite was launched on 23 June 2015, and the system provides freely available data with global coverage of the Earth's land surface with a revisit time of 5 days. The sensor collects data in 13 spectral bands with spatial resolutions ranging from 10 m–60 m. For this study, we used the four bands (blue, green, red and NIR) with 10 m resolution and included all

available cloud free imagery from 29 April to 26 September 2016 (see list of images and further details in Supplementary Table S2). The Sentinel-2 data was atmospherically corrected to a Bottom-Of-Atmosphere reflectance dataset using the 6SV model (Kotchenova et al., 2006) with a MODIS-based atmospheric characterization (Ju et al., 2012). For each image in the time series, average reflectances of the archaeological sites and surrounding reference areas were calculated for each band. We also calculated the Normalised Difference Vegetation Index (NDVI), an indicator related to vegetation productivity and one of the most commonly used spectral vegetation indices (Masini and Lasaponara, 2017; Pettorelli et al., 2005). NDVI is derived from the reflectance ratio of the red and NIR band (NDVI = NIR − red / NIR + red). Discrimination between specific areas (i.e. archaeological sites vs. reference areas) is shown in Supplementary Fig. S1.

2.5.3. Very high resolution (VHR) satellite imagery

To investigate the potential of using optical satellite imagery for monitoring archaeological sites, we included very high resolution (VHR) Pléiades-1 A/B data in the study (see list of images in Supplementary Table S2). Pléiades-1 A/B is a commercial sensor operated by Centre National d'Etudes Spatiales (CNES) with a spatial resolution of 2 m in four multi-spectral bands (blue, green, red and NIR) and of 0.5 m in one panchromatic band. The Pléiades data was atmospherically corrected to a Bottom-Of-Atmosphere reflectance dataset using the same procedure as described for the Sentinel-2 data. For analysis, the four multi-spectral bands were used both in its original 2 m spatial resolution and in a pan-sharpened version with a resolution of 0.5 m using the NNDiffuse Pan Sharpening algorithm in ENVI (Harris Geospatial Solution, Boulder, USA).

2.5.4. Statistical analysis

All parameters related to soil chemistry and vegetation biomass were subjected to an analysis of variance (ANOVA). To make data conform to normality, several parameters were log-transformed (noted in Supplementary Table S3). The models were validated with residual and normal Q-Q plots. We used a two-way design with area type as one factor (with two levels; archaeological site and reference area) and study site as the other factor (with five levels; Kangeq, Ersaa, Qoornoq, Iffiartafik, Sandnes). The models were tested for main effects (area type and study sites) and the interaction between these. As we focus on the difference between area type (archaeological site vs. reference area), the model was also tested for main effects using LS means despite interactions between area type and study sites. This was done for the parameters above- and below-ground biomass, NO_3, NH_4, PO_4, DON, TDN, DOC, C—N ratio and $\delta^{15}N$, where mean values at archaeological sites across all five study sites were all higher/lower than the reference areas (with exception of below-ground biomass at Iffiartafik and DOC at Qoornoq). The results presented in Table 1 and Supplementary Table S4 are untransformed mean values, whereas the denoted p-values derive from models based on data that may be log-transformed (noted in Supplementary Table S3). The observations of plant species composition (pin-point data) were subjected to a principal component (PC) analysis. The extracted PCs were analysed with ANOVA as above. All statistical analyses were made in R version 3.4.2.

3. Results

3.1. Site specific meteorological conditions

The measured air and surface temperatures confirm that the sites are located along a climate gradient with a marked increase in seasonal variation from west to east, travelling from the outer fjord to the inner fjord (Fig. 2). This is further emphasized by the number of thawing degree days (TDD) and freezing degree days (FDD) ranging from ~1500 FDD and ~900 TDD in the inner fjord (Sandnes and Iffiartrafik) to ~1200 FDD and ~520 TDD in the outer fjord (Kangeq and Ersaa). There is also a marked difference in the amount of rain observed during the frost-free period, with inland sites only receiving 64 mm compared to 260 mm on the outer coast (Fig. 2). The overall spatial trends observed with regards to air temperatures and precipitation rates are similarly reflected in the upper parts of the soil, with higher summer soil temperatures and drier conditions observed at sites in the inner fjord (Fig. 2; Supplementary Fig. S2). Comparison with air temperatures from two official meteorological stations in the outer fjord (Nuuk) and inner fjord (Kapisillit) shows that the study year (2016/17) fell within the normal temperature range observed during the last 15 years (Supplementary Fig. S3).

Table 1
Depth-integrated soil content (0–35 cm) of NO_3-N, NH_4-N, Olsen-P and below-ground biomass. Also, above-ground biomass is given. Values are means (±SE) of six replicate plots from archaeological sites (grey-shaded) and surrounding reference areas. Significant differences (ANOVA, $n = 60$) between archaeology and reference areas are denoted by the values *($p < 0.05$), **($p < 0.01$),***($p < 0.001$).

	NO_3 (g/m²)	NH_4 (g/m²)	Olsen-P (g/m²)	Biomass above (kg/m²)	Biomass below (kg/m²)
Kangeq	0.51±0.15***	0.47±0.06*	20.89±2.32***	0.4±0.07**	1.34±0.29*
	0.04±0.01	0.16±0.04	2.07±0.43	0.15±0.03	0.75±0.15
Ersaa	0.18±0.03***	0.65±0.14***	14.85±3.58***	0.27±0.05	1.43±0.08***
	0.03±0	0.04±0.02	2.05±0.37	0.17±0.03	0.38±0.03
Qoornoq	0.53±0.15***	0.85±0.2**	29.01±4.93***	0.46±0.12*	1.2±0.14*
	0.04±0.01	0.07±0.02	3.14±0.6	0.17±0.03	0.69±0.13
Iffiartafik	0.44±0.08***	0.8±0.12	12.51±2.4*	0.59±0.13***	0.93±0.3
	0.03±0.01	0.41±0.14	4.39±0.7	0.13±0.01	1.26±0.22
Sandnes	0.41±0.09	0.8±0.13	18.21±3.16	0.34±0.08	1.94±0.29*
	0.21±0.05	0.7±0.15	9.77±1.76	0.2±0.04	0.94±0.1
All sites	0.41±0.06***	0.71±0.07***	19.09±1.88***	0.41±0.05***	1.37±0.13***
	0.07±0.02	0.28±0.02	4.29±0.68	0.17±0.01	0.81±0.08

3.2. Vegetation

Plot scale observations of the distribution of plants show a marked difference between archaeological sites and surrounding reference areas (Fig. 3A–B). Archaeological sites are highly dominated by graminoids and horsetail, whereas reference areas show a more diverse plant cover dominated by deciduous shrubs, evergreen shrubs, graminoids and mosses. The same conclusion is reached by the principal component (PC) analysis of the pinpoint data (Fig. 3C–D), which demonstrates that archaeological sites and surrounding reference areas are significantly different (PC1, $p < 0.001$). Similarly, approximately two times more above- and below-ground biomass is found on archaeological sites compared to reference areas (Table 1; Supplementary Fig. S4). With all study sites combined, the difference is highly significant ($p < 0.001$).

For archaeological sites, no general trends are found for plant cover percentage, plant species composition and biomass (above- and below-ground) in relation to the climate variations found along the west-east transect (Fig. 3A–B; Table 1). For the surrounding reference areas, a general trend of increase in plant cover is observed stretching from the outer fjord (170% at Kangeq) to the inner fjord (332% at Sandnes). As one travels from the coast to the inland, deciduous shrubs and graminoids are observed to increase as evergreen shrubs decrease. The trend is, however, not reflected in the quantity of above- and below-ground biomass. (Table 1).

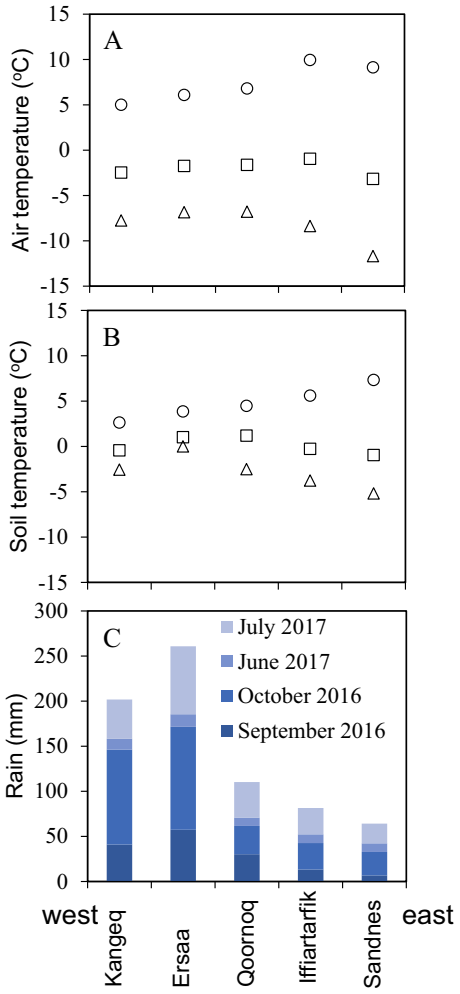

Fig. 2. Meteorological conditions at the five study sites along the west-east transect. A and B show air and soil (10 cm depth) temperatures. Open squares are mean temperatures in the period 1 September 2016–31 July 2017. Open circles are mean summer temperatures (June–July 2017). Open triangles are mean winter temperatures (December 2016–February 2017). C shows precipitation in the frost-free period.

3.3. Soil chemistry

Fig. 4 shows the measured soil content of water extractable nitrate (NO_3-N) and ammonium (NH_4-N) and Olsen extractable phosphorus (Olsen P) at the five study sites at 0–5, 10–15, 20–25 and 30–35 cm depths. In all cases, the depth-integrated nutrient levels are higher in samples from the archaeological sites than from the surrounding reference areas (Table 1), statistically significant at Kangeq, Ersaa, Qoornoq and Iffiartafik (except for NH_4-N), but not at Sandnes (p-values in Table 1). When all study sites are combined the pattern is highly significant ($p < 0.001$). Soil dissolved organic nitrogen (DON), total dissolved nitrogen (TDN), dissolved organic carbon (DOC), C—N ratio, $\delta^{15}N$, $\delta^{13}C$, water content and pH are presented in Supplementary Figs. S5–7 and Table S4. Significantly higher values for DON and TDN are found in samples from archaeological sites when compared to reference areas ($p < 0.001$), but not for DOC. The C—N ratios are at the same level (~13) in all archaeological samples and vary from 13 to 26 in reference samples. For all sites combined, there is a significant difference in C—N ratios between archaeological and reference samples ($p < 0.001$). For all study sites, the soil $\delta^{15}N$ values are significantly higher in archaeological samples ($p < 0.001$), while there is no difference in soil $\delta^{13}C$ values. For Qoornoq, Iffiartafik and Sandnes, water content (vol%) is consistent in samples across archaeological sites and reference areas whereas, at Ersaa and Kangeq, the water content is significantly higher in reference samples. For both archaeological sites and reference areas, pH varies between 4.5 and 6 with no significant trends.

3.4. Remote sensing investigations

To complement the plot scale investigations, vegetation cover was mapped at the site scale using UAV-based RGB image mosaics (Fig. 5; Supplementary Fig. S8). The areas of the archaeological sites were defined based on the distinct plant characteristics found in the plot scale investigations in combination with the presence of archaeological features such as ruins, middens or other archaeological indicators. The vegetation maps support the findings from the plot scale investigations and demonstrate that archaeological sites are dominated by graminoids, whereas the vegetation cover in the reference areas is more variable with mostly low vegetation species found in the mid- and outer fjord (Kangeq, Ersaa, Qoornoq) versus a dominance of deciduous shrubs in the inner fjord (Iffiartafik and Sandnes).

Because the plot scale and UAV investigations only represent a snapshot in time, Sentinel-2 imagery was used to investigate the spectral properties throughout the entire growing season. Fig. 6 shows the reflectance in the Sentinel-2 bands with 10 m spatial resolution (Blue, Green, Red and NIR) throughout the growing season at Kangeq and Iffiartafik (the remaining sites are shown in Supplementary Fig. S9). From the Sentinel-2 time series, it is observed that the spectral reflectance is generally higher at the archaeological sites compared to the reference areas. NDVI increases at the beginning of the growing season and peaks at the end of July for both archaeological sites and surrounding reference areas. The difference in NDVI between archaeological sites and reference areas shows high variability throughout the growing season and is inconsistent across the study sites (Fig. 6; Supplementary Fig. S9). By contrast, the NIR band highlights a distinct and consistent difference between archaeological sites and reference areas throughout the entire growing season across all study sites (Fig. 6; Supplementary Fig. S9). The NIR difference at Iffiartafik is illustrated in detail in Fig. 7, with imagery representing different spatial resolutions (UAV mosaic, Pléiades, Sentinel-2).

4. Discussion

4.1. Vegetation and soil characteristics

We investigated the vegetation on five contrasting archaeological sites in terms of age, depositional and climatic conditions. Results of the study show a clear difference between archaeological sites and the surrounding reference areas in both plant species composition and above- and below-ground biomass. At the archaeological sites, the vegetation is observed as homogeneous and dominated by graminoids whereas the reference areas are more heterogeneous (deciduous and evergreen shrubs, graminoids and mosses) as seen in Fig. 3. Furthermore, above- and below-ground biomasses at the archaeological sites average about twice as high as in the reference areas (Table 1). The differences in vegetation cover result in different spectral properties; archaeological sites appear to have a similar or higher reflectance in the visual part of the spectrum (Blue, Green, Red) and a consistently higher reflectance in the NIR part of the spectrum throughout the growing season compared to the surrounding areas (Fig. 6; Supplementary Fig. S9). As NDVI is a widely used indicator of vegetation productivity (Pettorelli et al., 2005), it was expected that the significantly higher above-ground biomass at the archaeological sites also resulted in a higher NDVI by the time of the field investigations in August. This is, however, not the case at Iffiartafik and Sandnes (Fig. 6; Supplementary Fig. S9C) because of the way NDVI is calculated. Here, the difference observed in the NIR band is equalized by the difference observed in the Red band. Thus, the observed vegetation differences between archaeological sites and the

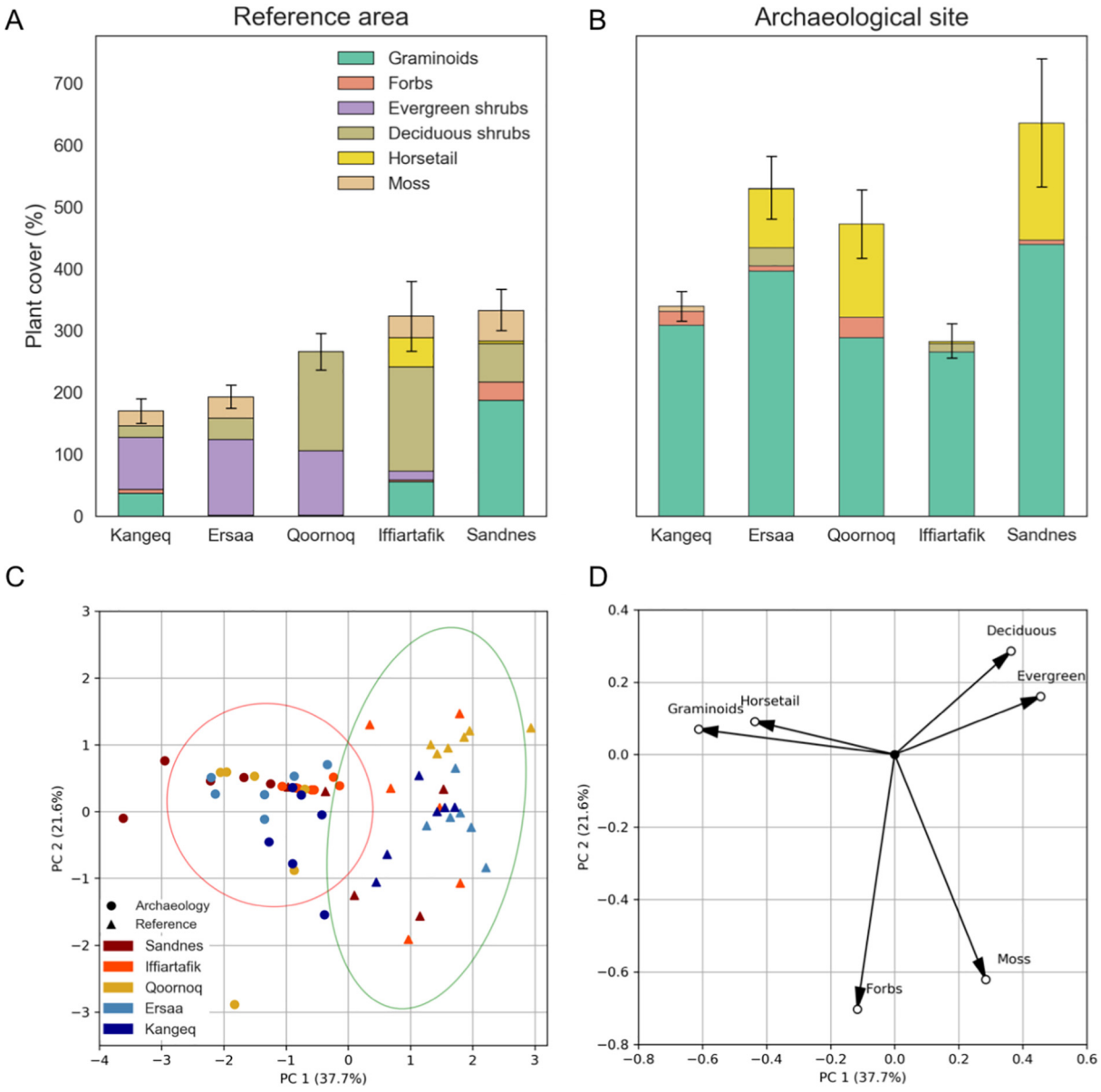

Fig. 3. A–B show plant functional groups based on pinpoint data from the plot scale investigations at five archaeological sites and surrounding reference areas (±SE). C–D show a principal component (PC) analysis on the pinpoint data. The areas outlined in C by the red and the green ellipses illustrate the 95% confidence interval of PC 1 and PC 2 for archaeological and reference plots respectively. The loading in D shows how the plant functional groups influence the position of each point in C.

surrounding areas are related to differences in the spectral properties, but not necessarily to NDVI.

It is well-known that past human activities can have a significant impact on plant species composition and the functioning of tundra ecosystems and that these human 'footprints' can be evident for decades and even centuries (Derry et al., 1999; Forbes, 1996; Freschet et al., 2014). In particular, increased soil nutrient availability is known to alter the competitive balance in the plant community (Lambers and Poorter, 1992). Our results show that the content of plant available nutrients (NO_3, NH_4, Olsen P) is much higher in archaeological deposits than in the surrounding reference areas (Table 1). Human activities often result in the accumulation of nitrogen and phosphorus in the area of occupation. Especially phosphorus-hotspots are widely used in archaeology as an indicator of human activity as the accumulated phosphorus tends to remain constant over time (Craddock et al., 1985; Sjöberg, 1976). Additionally, a high $\delta^{15}N$ fraction in plants growing on archaeological sites is also recognized as a long-term signature of past human activity (Commisso and Nelson, 2008). The significantly higher content of phosphorus and $\delta^{15}N$ in the samples from the archaeological sites compared to the reference areas (Table 1, Supplementary Table S4) confirms that the higher nutrient content is closely related to past time human activity.

Our reference plots were located away from the archaeological sites but were still relatively close to areas of past human activity. Consequently, the distance may have been too short to reach completely undisturbed conditions. This may explain the relatively high values of plant available nutrients found in the reference area at Sandnes (Fig. 4, Table 1). Here, the Norse practiced livestock farming approx. 300 years ago (McGovern et al., 1996) and may therefore have extensively impacted the surrounding area. Thus, the differences presented here should rather be seen as a conservative estimate of the complete spectrum of differences between the human influenced archaeological sites and the undisturbed natural environment.

For reference areas, the plant cover becomes denser and the functional plant groups shifts from evergreen shrubs to deciduous shrubs and graminoids when travelling from the cold and wet outer fjord to

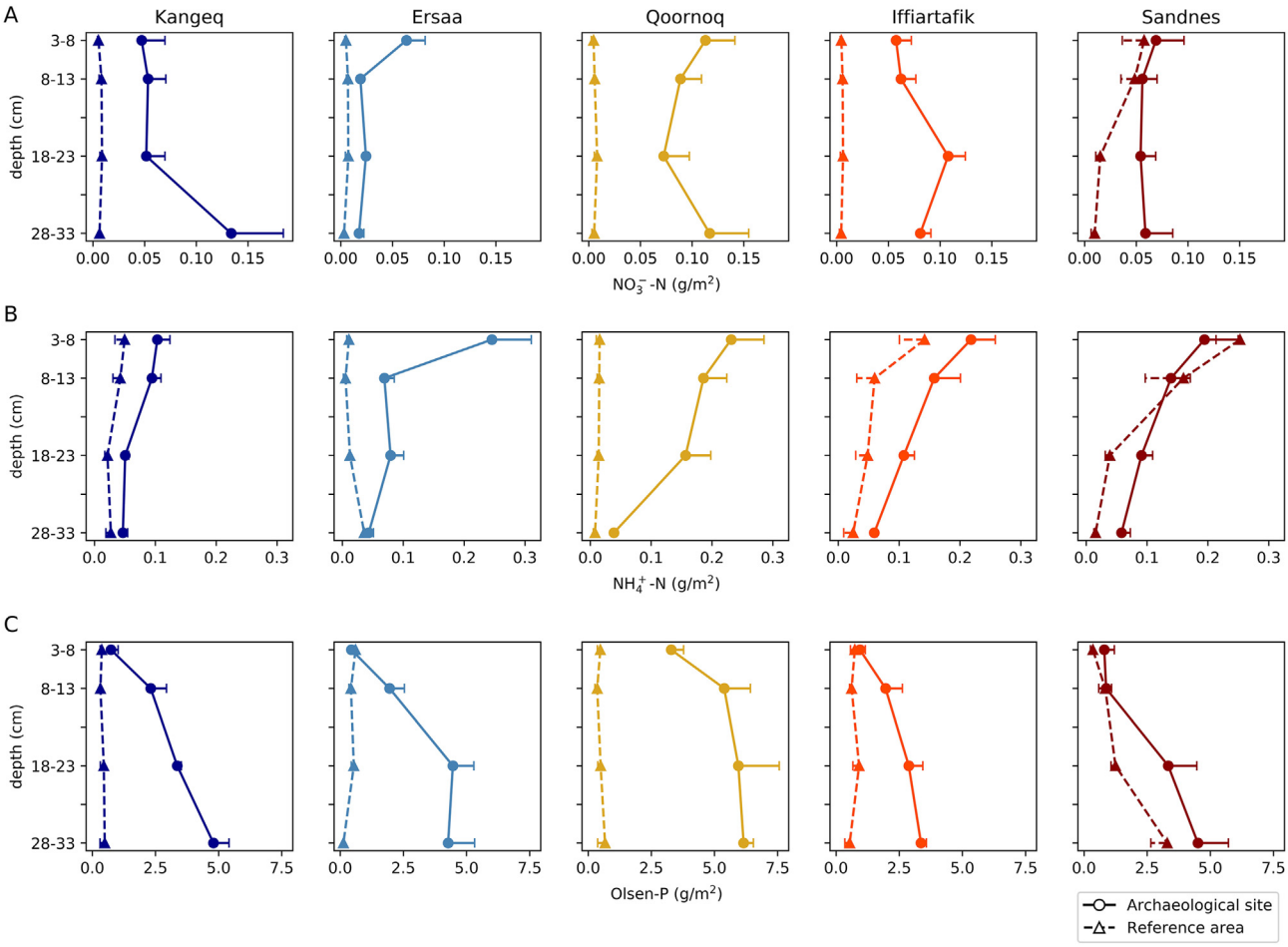

Fig. 4. Water extractable nitrate (A) and ammonium (B) and Olsen extractable phosphorus (C) in soil samples from archaeological sites and reference areas at 3–8, 8–13, 18–23, and 28–33 cm depths at all study sites. The plotted values are means of six replicate plots (±SE). If SE lines are not visible, they are smaller than the symbol.

the warmer and drier inner fjord. However, no response to the regional climatic variations is seen for the archaeological sites. None of the sites showed signs of the vegetation growth being limited by low water supply (Supplementary Table S4). This suggests that the vegetation at the archaeological sites is mainly controlled by the high content of plant available nutrients rather than the local climate. Based on the results of this study, we cannot definitively conclude whether nitrogen or phosphorus is the most important factor for increased plant growth and the observed shift in species composition towards dominance of graminoids at the archaeological sites. However, both the addition of nitrogen alone and, in particular, nitrogen in combination with phosphorus has previously been shown to promote plant growth in the Arctic (Elser et al., 2007; Schmidt et al., 1997).

The consistency of improved conditions for vegetation growth across all archaeological sites and the link to higher nutrient levels further suggest that future soil-vegetation interactions at archaeological sites may not be similar to the soil-vegetation interactions of the natural environment. The potential for increased nutrient turnover with climate warming may be extraordinarily high at archaeological sites. This could further increase both above- and below-ground biomass with negative consequences for preservation conditions at archaeological sites.

4.2. Monitoring vegetation at archaeological sites

The observed difference in vegetation, soil characteristics and climatic response between the archaeological sites and the surrounding areas show that archaeological sites are fundamentally different from the natural environment. Consequently, existing studies on the greening of the Arctic (Elmendorf et al., 2012; Epstein et al., 2012; Jia et al., 2003; Myers-Smith et al., 2015) may not be directly applicable to archaeological sites. Hollesen et al. (2018) currently estimate that the Arctic may contain at least 180,000 archaeological sites. Very few of these sites have been investigated and little is known about their current state of preservation. The high number of sites and the logistical challenges of working in the Arctic make field-based vegetation surveys an extremely difficult and costly approach for evaluating the threat of vegetation on archaeological sites. Instead, the potential of applying methods based on Remote Sensing data including satellite imagery provides a reasonable alternative and could greatly improve knowledge of changing vegetation patterns that may be affecting the preservation conditions at archaeological sites.

For example, in a study from Northern Norway, Landsat satellite imagery was used with success to detect archaeological sites threatened by vegetation. However, the coarse spatial resolution (30 m) of the Landsat imagery was reported to limit the applicability (Barlindhaug et al., 2007). The new Sentinel-2 imagery has been emphasized to hold a potential for archaeological prospection due to the improved spatial resolution of 10 m and a revisit time of only 5 days (Agapiou et al., 2014; Tømmervik et al., 2010). Our results confirm this and show that Sentinel-2 imagery is a useful tool for vegetation monitoring of even small archaeological sites with a size of 50 × 50 m (the approximate size of the investigated archaeological sites in this study). The spatial resolution of 10 m in the visual and near-infrared bands permits monitoring of the overall vegetation status at the site level using a vegetation index such as NDVI. Furthermore, the revisit time of five days permits the elaboration of seasonal time series of observations (Fig. 6). For

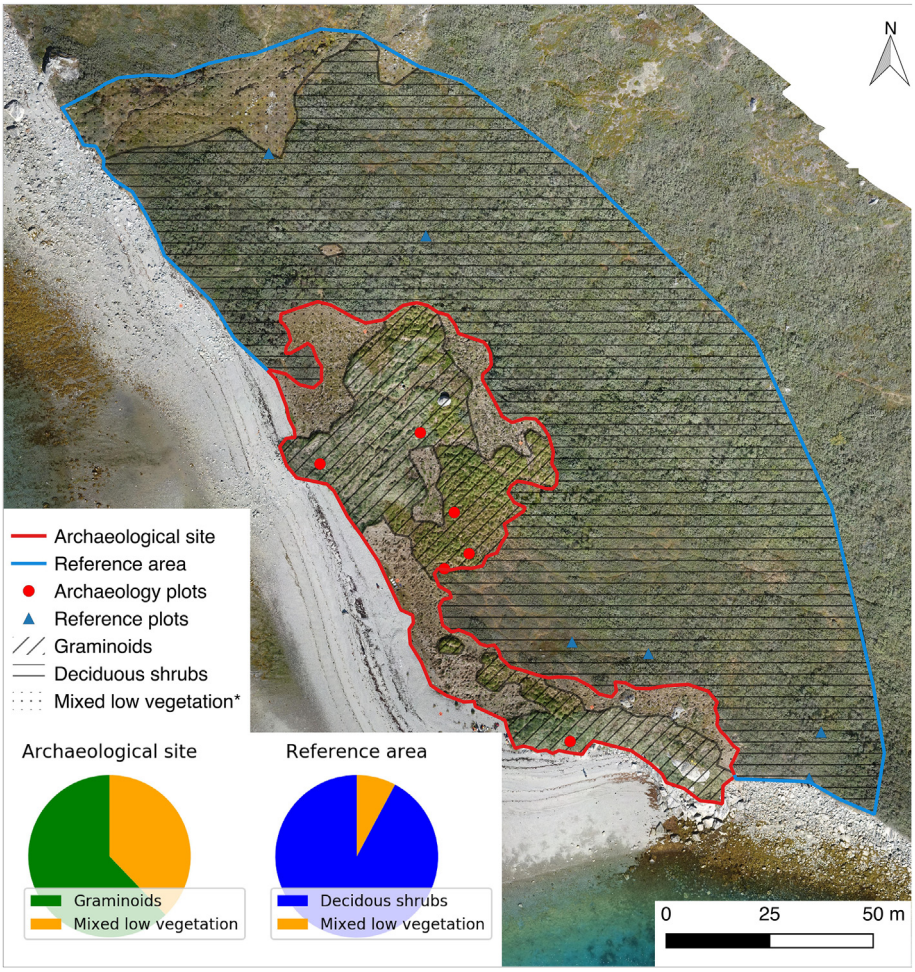

Fig. 5. Vegetation cover at Iffiartafik derived from the UAV-based RGB mosaic. The class 'Mixed low vegetation' includes graminoids, deciduous and evergreen shrubs and moss.

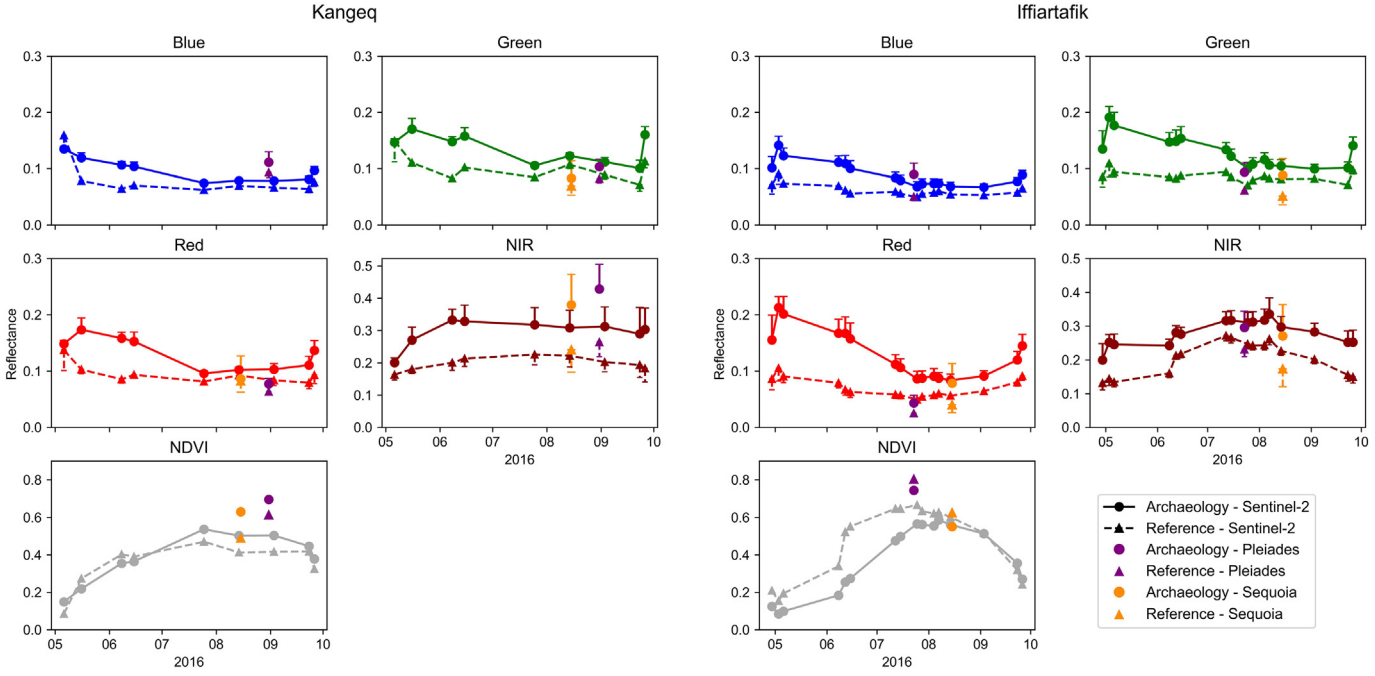

Fig. 6. Spectral reflectance and NDVI at archaeological sites and reference areas based on the Sentinel-2 10 m spatial resolution bands (blue, green, red and NIR) throughout the growing season May–September 2016. Reflectance is also shown from the UAV-based multispectral observations (Parrot Sequoia) and from the VHR Pléiades satellite imagery for comparison. Plotted values are means of pixel values. The Sentinel-2 bands are shown ± one standard deviation.

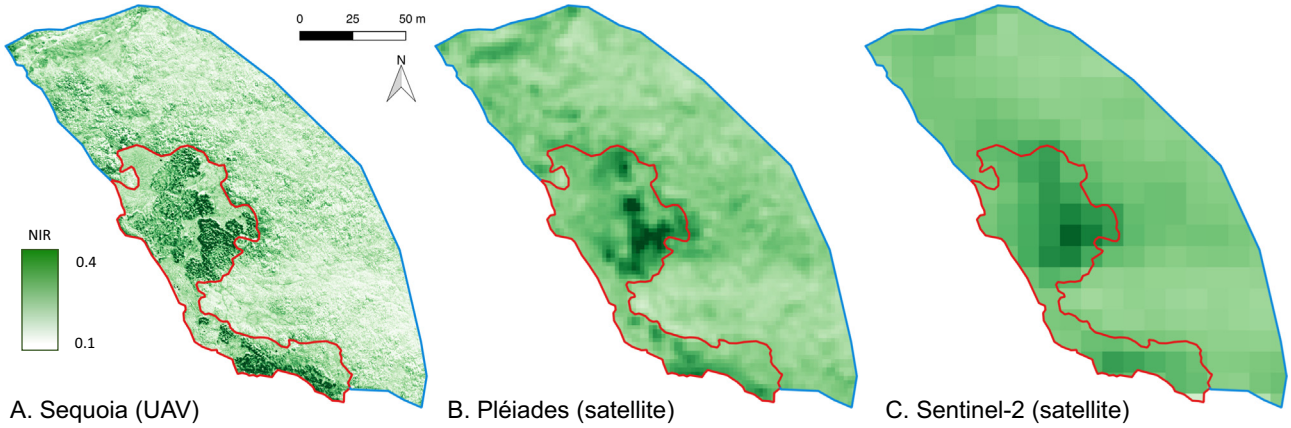

Fig. 7. The archaeological site at Iffiartafik (within the red boundary) seen in the NIR band from three different multi-spectral sensors: A. Parrot- Sequoia with a spatial resolution of 8.2 cm acquired 15 August 2016, B. Pléiades with a resolution of 2 m acquired on 23 July 2016, C. Sentinel-2 with a resolution of 10 m acquired on 28 July 2016.

mapping the detailed spectral variations within each site, the Sentinel-2 time series can be supplemented by VHR satellite data similar to the Pléiades imagery used in this study (Fig. 7). Thus, the recent availability of higher resolution satellite data permits larger scale vegetation monitoring at archaeological sites now and in the future. However, back in time, it is more difficult to conclude to which degree the documented greening of the Arctic also occurred on the archaeological sites. Dendrochronological studies have been widely used to investigate the climate response of deciduous shrubs (Hollesen et al., 2015; Myers-Smith et al., 2015) and heath vegetation (Weijers et al., 2017) in the Arctic. This could also be a useful method at archaeological sites.

4.3. Detection of archaeological sites

Observed differences in the spectral properties of archaeological sites and the surrounding area have great potential for detecting unknown archaeological sites using satellite imagery and have shown promising results (Grøn et al., 2011; Keeney and Hickey, 2015; Masini and Lasaponara, 2017; Masini et al., 2018). In Greenland, as of August 2018, approximately 6000 sites are registered in Nunniffiit, the national database of cultural heritage monuments and properties (http://nunniffiit.natmus.gl – last visited August 2018). It is also estimated that a large number of undiscovered sites still exist in the many parts

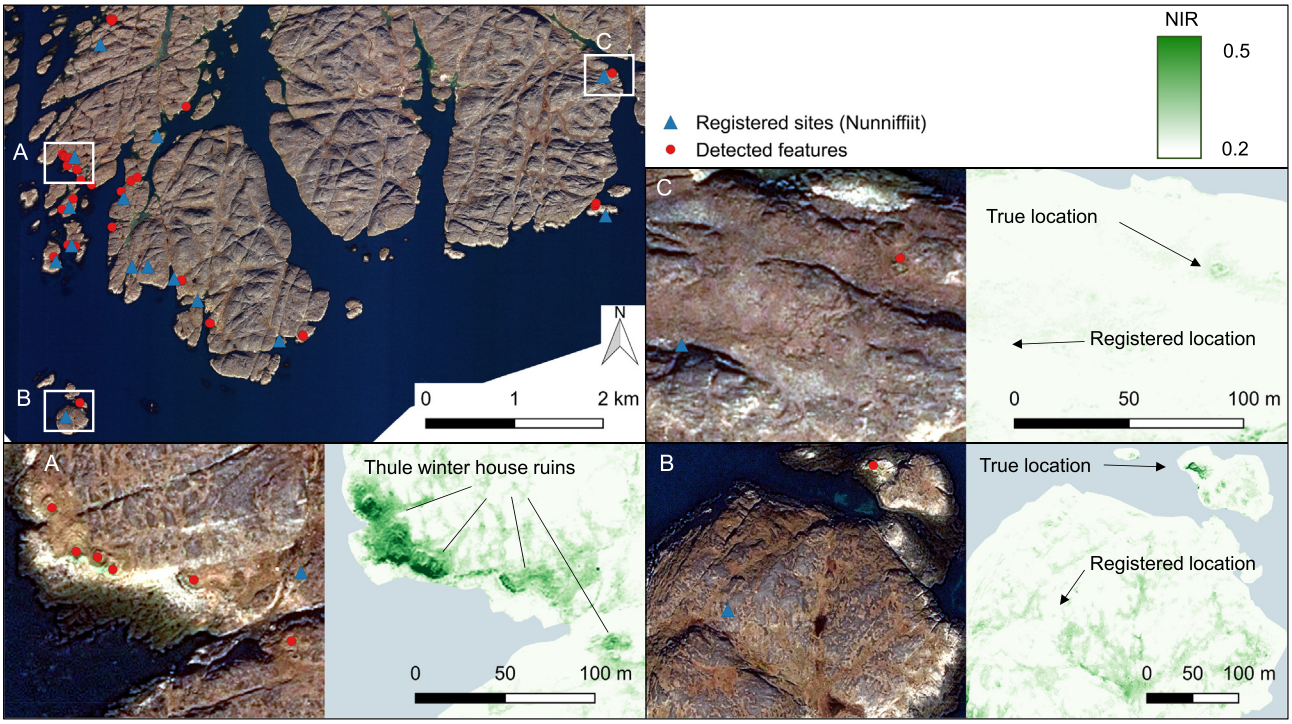

Fig. 8. Pléiades satellite image of the Kangeq area, where 15 archaeological sites are registered in the Greenlandic national database of cultural heritage monuments and properties (Nunniffiit). A manual search of the imagery using RGB and NIR revealed 36 potential archaeological sites or features. Zoom window A shows an example of Thule winter house ruins detected in the Pléiades imagery. Zoom window B and C are examples of misplaced sites in the spatial registry.

of the country. As climate change has marked implications for the preservation of archaeological sites in the Arctic (Hollesen et al., 2018), discovering these sites is extremely important before they are lost. VHR satellite imagery offers one potential tool for desk-based archaeological prospection in Greenland that could be prioritized for future ground survey.

To investigate the potential for using satellite imagery for site detection, we used the acquired Pléiades data (pan-sharpened RGB and NIR) and focused on an area near the study site Kangeq. Although NDVI or similar vegetation indices are widely used for site detection in optical imagery (Masini and Lasaponara, 2017), we used the NIR band because the contrast between archaeological sites and reference areas was higher and more robust over the growing season compared to NDVI (Fig. 6). The Nunniffiit database shows that 15 archaeological sites are registered in this area. However, we identified a total of 36 sites or features in the satellite imagery (Fig. 8). The sites cannot be compared one-to-one because the registered sites may refer to several features. It is therefore not possible to determine if any of the detected features are unknown without ground-truthing. The analysis also shows that many of the registered sites are misplaced in the spatial registry by >100 m. The results thus demonstrate the great potential for using satellite imagery to search for undiscovered archaeological sites and for improving the spatial registry of already registered sites.

5. Conclusion

We observed that the vegetation cover at five contrasting archaeological sites in Southwest Greenland is homogenous and dominated by graminoids, despite differences in climatic conditions. The vegetation on the archaeological sites differs significantly from the vegetation in the surrounding natural areas, observed as more heterogeneous and with less above- and below-ground biomass. We conclude that these differences in vegetation are associated with a markedly higher content of plant available nutrients (NO_3, NH_4 and Olsen P) found on the archaeological sites as a result of past human activity. These 'footprints' from the past are reflected in the spectral signal captured in UAV and satellite imagery allowing for detection of archaeological sites using remote sensing.

The 'hotspots' of vegetation and nutrients found on the archaeological sites suggest that soil-vegetation interactions at archaeological sites are markedly different from the natural environment. Furthermore, vegetation at the archaeological sites responds differently to climatic variations. Consequently, the long-term vulnerability of buried archaeological remains cannot be based on existing projections of Arctic vegetation change. As a result, we stress the importance of performing vegetation assessments specifically on archaeological sites in relation to climate change. For large-scale vegetation monitoring of archaeological sites, we suggest remote sensing as a highly cost-effective and productive approach. This study shows that new satellite constellations such as Sentinel-2 offers data with a sufficient temporal and spatial resolution to monitor vegetation at even small sites.

Acknowledgement

We gratefully acknowledge financial support from VELUX FONDEN (33813) and the Danish National Research Foundation (Center for Permafrost, CENPERM DNRF100).

Appendix A. Supplementary data

Supplementary data to this article can be found online at https://doi.org/10.1016/j.scitotenv.2018.11.018.

References

Agapiou, A., Alexakis, D., Sarris, A., Hadjimitsis, D., 2014. Evaluating the potentials of Sentinel-2 for archaeological perspective. Remote Sens. 6, 2176–2194. https://doi.org/10.3390/rs6032176.

Barlindhaug, S., Holm-Olsen, I.M., Tømmervik, H., 2007. Monitoring archaeological sites in a changing landscape–using multitemporal satellite remote sensing as an 'early warning' method for detecting regrowth processes. Archaeol. Prospect. 14, 231–244. https://doi.org/10.1002/arp.307.

Commisso, R.G., Nelson, D.E., 2008. Correlation between modern plant $\delta^{15}N$ values and activity areas of medieval Norse farms. J. Archaeol. Sci. 35, 492–504. https://doi.org/10.1016/j.jas.2007.05.012.

Craddock, P.T., Gurney, D., Pryor, F., Hughes, M.J., 1985. The application of phosphate analysis to the location and interpretation of archaeological sites. Archaeol. J. 142, 361–376. https://doi.org/10.1080/00665983.1985.11021068.

Crow, P., Moffat, A.J., 2005. The management of the archaeological resource in UK wooded landscapes: an environmental perspective. Conserv. Manag. Archaeol. Sites 7, 103–116. https://doi.org/10.1179/135050305793137512.

Delgado, A., Torrent, J., 1997. Phosphate-rich soils in the European Union: estimating total plant-available phosphorus. Eur. J. Agron. 6, 205–214. https://doi.org/10.1016/S1161-0301(96)02048-5.

Derry, A.M., Kevan, P.G., Rowley, S.D.M., 1999. Soil nutrients and vegetation characteristics of a Dorset/Thule site in the Canadian Arctic. Arctic 52, 204–213. https://doi.org/10.14430/arctic923.

Elberling, B., Matthiesen, H., Jørgensen, C.J., Hansen, B.U., Grønnow, B., Meldgaard, M., et al., 2011. Paleo-Eskimo kitchen midden preservation in permafrost under future climate conditions at Qajaa, West Greenland. J. Archaeol. Sci. 38, 1331–1339. https://doi.org/10.1016/j.jas.2011.01.011.

Elmendorf, S.C., Henry, G.H.R., Hollister, R.D., Björk, R.G., Boulanger-Lapointe, N., Cooper, E.J., et al., 2012. Plot-scale evidence of tundra vegetation change and links to recent summer warming. Nat. Clim. Chang. 2, 453. https://doi.org/10.1038/nclimate1465.

Elser, J.J., Bracken, M.E.S., Cleland, E.E., Gruner, D.S., Harpole, W.S., Hillebrand, H., et al., 2007. Global analysis of nitrogen and phosphorus limitation of primary producers in freshwater, marine and terrestrial ecosystems. Ecol. Lett. 10, 1135–1142. https://doi.org/10.1111/j.1461-0248.2007.01113.x.

Epstein, H.E., Raynolds, M.K., Walker, D.A., Bhatt, U.S., Tucker, C.J., Pinzon, J.E., 2012. Dynamics of aboveground phytomass of the circumpolar Arctic tundra during the past three decades. Environ. Res. Lett. 7. https://doi.org/10.1088/1748-9326/7/1/015506.

Forbes, B.C., 1996. Plant Communities of Archaeological Sites, Abandoned Dwellings, and Trampled Tundra in the Eastern Canadian Arctic: A Multivariate Analysis. Vol. 49: 14. https://doi.org/10.14430/arctic1192.

Forbes, B.C., Ebersole, J.J., Strandberg, B., 2001. Anthropogenic disturbance and patch dynamics in circumpolar Arctic ecosystems. Conserv. Biol. 15, 954–969. https://doi.org/10.1046/j.1523-1739.2001.015004954.x.

Freschet, G.T., Östlund, L., Kichenin, E., Wardle, D.A., 2014. Aboveground and belowground legacies of native Sami land use on boreal forest in northern Sweden 100 years after abandonment. Ecology 95, 963–977. https://doi.org/10.1890/13-0824.1.

Grøn, O., Palmér, S., Stylegar, F.-A., Esbensen, K., Kucheryavski, S., Aase, S., 2011. Interpretation of archaeological small-scale features in spectral images. J. Archaeol. Sci. 38, 2024–2030. https://doi.org/10.1016/j.jas.2009.11.023.

Grønnow, B., 1994. Qeqertasussuk-the archaeology of a frozen Saqqaq site in Disko Bugt, West Greenland. Threads of Arctic Prehistory: Papers in Honour of William E. Taylor Jr.Canadian Museum of Civilization, Ottawa, Canada, pp. 197–238

Gyssels, G., Poesen, J., Bochet, E., Li, Y., 2005. Impact of plant roots on the resistance of soils to erosion by water: a review. Prog. Phys. Geogr. Earth Environ. 29, 189–217. https://doi.org/10.1191/0309133305pp443ra.

Hollesen, J., Buchwal, A., Rachlewicz, G., Hansen, B.U., Hansen, M.O., Stecher, O., et al., 2015. Winter warming as an important co-driver for Betula nana growth in western Greenland during the past century. Glob. Chang. Biol. 21, 2410–2423. https://doi.org/10.1111/gcb.12913.

Hollesen, J., Matthiesen, H., Møller, A.B., Westergaard-Nielsen, A., Elberling, B., 2016. Climate change and the loss of organic archaeological deposits in the Arctic. Sci. Rep. 6, 28690. https://doi.org/10.1038/srep28690.

Hollesen, J., Callanan, M., Dawson, T., Fenger-Nielsen, R., Friesen, T.M., Jensen, A.M., et al., 2018. Climate change and the deteriorating archaeological and environmental archives of the Arctic. Antiquity 92, 573–586. https://doi.org/10.15184/aqy.2018.8.

IPCC, 2013. Annex V: contributors to the IPCC WGI Fifth assessment report. In: Stocker, T.F., Qin, D., Plattner, G.-K., Tignor, M., Allen, S.K., Boschung, J., et al. (Eds.), Climate Change 2013: The Physical Science Basis. Contribution of Working Group I to the Fifth Assessment Report of the Intergovernmental Panel on Climate Change. Cambridge University Press, Cambridge, United Kingdom and New York, NY, USA, pp. 1477–1496 https://doi.org/10.1017/CBO9781107415324.

Jia, G.J., Epstein, H.E., Walker, D.A., 2003. Greening of arctic Alaska, 1981–2001. Geophys. Res. Lett. 30. https://doi.org/10.1029/2003GL018268.

Ju, J., Roy, D.P., Vermote, E., Masek, J., Kovalskyy, V., 2012. Continental-scale validation of MODIS-based and LEDAPS Landsat ETM+ atmospheric correction methods. Remote Sens. Environ. 122, 175–184. https://doi.org/10.1016/j.rse.2011.12.025.

Keeney, J., Hickey, R., 2015. Using satellite image analysis for locating prehistoric archaeological sites in Alaska's Central Brooks Range. J. Archaeol. Sci. Rep. 3, 80–89. https://doi.org/10.1016/j.jasrep.2015.05.022.

Kotchenova, S.Y., Vermote, E.F., Matarrese, R., Klemm, J.F.J., 2006. Validation of a vector version of the 6S radiative transfer code for atmospheric correction of satellite data. Part I: path radiance. Appl. Opt. 45, 6762–6774. https://doi.org/10.1364/AO.45.006762.

Lambers, H., Poorter, H., 1992. In: Begon, M., Fitter, A.H. (Eds.), Inherent Variation in Growth Rate Between Higher Plants: A Search for Physiological Causes and Ecological Consequences. Advances in Ecological Research Vol. 23. Academic Press, pp. 187–261. https://doi.org/10.1016/S0065-2504(08)60148-8.

Lantuit, H., Overduin, P.P., Couture, N., Wetterich, S., Aré, F., Atkinson, D., et al., 2012. The Arctic coastal dynamics database: a new classification scheme and statistics on Arctic permafrost coastlines. Estuar. Coasts 35, 383–400. https://doi.org/10.1007/s12237-010-9362-6.

Lisci, M., Monte, M., Pacini, E., 2003. Lichens and higher plants on stone: a review. Int. Biodeterior. Biodegrad. 51, 1–17. https://doi.org/10.1016/S0964-8305(02)00071-9.
Masini, N., Lasaponara, R., 2017. Sensing the past from space: approaches to site detection. In: Masini, N., Soldovieri, F. (Eds.), Sensing the Past: From Artifact to Historical Site. Springer International Publishing, Cham, pp. 23–60 https://doi.org/10.1007/978-3-319-50518-3_2.
Masini, N., Marzo, C., Manzari, P., Belmonte, A., Sabia, C., Lasaponara, R., 2018. On the characterization of temporal and spatial patterns of archaeological crop-marks. J. Cult. Herit. 32, 124–132. https://doi.org/10.1016/j.culher.2017.12.009.
McGovern, T.H., Amorosi, T., Perdikaris, S., Woollett, J., 1996. Vertebrate zooarchaeology of Sandnes V51: economic change at a Chieftain's farm in West Greenland. Arct. Anthropol. 33, 94–121. http://www.jstor.org/stable/40316414.
Meldgaard, M., 2004. Ancient Harp Seal Hunters of Disko Bay: Subsistence and Settlement at the Saqqaq Culture Site Qeqertasussuk (2400–1400 BC), West Greenland. Monographs on Greenland, Serie: Man & Society 30 pp. 1–189.
Myers-Smith, I.H., Elmendorf, S.C., Beck, P.S.A., Wilmking, M., Hallinger, M., Blok, D., et al., 2015. Climate sensitivity of shrub growth across the tundra biome. Nat. Clim. Chang. 5, 887. https://doi.org/10.1038/nclimate2697.
Olsen, S.R., Cole, C., Watanabe, F., Dean, L., 1954. Estimation of available phosphorus in soils by extraction with sodium bicarbonate. USDA Circular No. 939. United States Department Of Agriculture, Washington DC.
O'Rourke, M.J.E., 2017. Archaeological site vulnerability modelling: the influence of high impact storm events on models of shoreline Erosion in the Western Canadian Arctic. Open Archaeol. 3, 1–16. https://doi.org/10.1515/opar-2017-0001.
Parrot, 2017. SEQ-AN-01, Application Note: Pixel Value to Irradiance Using the Sensor Calibration Model. https://forum.developer.parrot.com/uploads/default/original/2X/3/383261d35e33f1f375ee49e9c7a9b10071d2bf9d.pdf.
Permafrost Subcommittee, 1988. Glossary of Permafrost and Related Ground-ice terms. Vol. 156. Associate Committee on Geotechnical Research, National Research Council of Canada, Ottawa. http://globalcryospherewatch.org/reference/glossary_docs/permafrost_and_ground_terms_canada.pdf.
Pettorelli, N., Vik, J.O., Mysterud, A., Gaillard, J.-M., Tucker, C.J., Stenseth, N.C., 2005. Using the satellite-derived NDVI to assess ecological responses to environmental change. Trends Ecol. Evol. 20, 503–510. https://doi.org/10.1016/j.tree.2005.05.011.
Rasmussen, M., Li, Y., Lindgreen, S., Pedersen, J.S., Albrechtsen, A., Moltke, I., et al., 2010. Ancient human genome sequence of an extinct Palaeo-Eskimo. Nature 463, 757–762. https://doi.org/10.1038/nature08835.
Sandweiss, D.H., Kelley, A.R., 2012. Archaeological contributions to climate change research: the archaeological record as a paleoclimatic and paleoenvironmental archive. Annu. Rev. Anthropol. 41, 371–391. https://doi.org/10.1146/annurev-anthro-092611-145941.
Schmidt, I.K., Michelsen, A., Jonasson, S., 1997. Effects on plant production after addition of labile carbon to Arctic/Alpine soils. Oecologia 112, 305–313. https://doi.org/10.1007/s004420050313.
Sjöberg, A., 1976. Phosphate analysis of anthropic soils. J. Field Archaeol. 3, 447–454. https://doi.org/10.1179/009346976791490493.
Smith, G.M., Milton, E.J., 1999. The use of the empirical line method to calibrate remotely sensed data to reflectance. Int. J. Remote Sens. 20, 2653–2662. https://doi.org/10.1080/014311699211994.
Swann, A.L., Fung, I.Y., Levis, S., Bonan, G.B., Doney, S.C., 2010. Changes in Arctic vegetation amplify high-latitude warming through the greenhouse effect. Proc. Natl. Acad. Sci. 107, 1295–1300. https://doi.org/10.1073/pnas.0913846107.
Tjelldén, A.K.E., Kristiansen, S.M., Matthiesen, H., Pedersen, O., 2015. Impact of roots and rhizomes on wetland archaeology: a review. Conserv. Manag. Archaeol. Sites 17, 370–391. https://doi.org/10.1080/13505033.2016.1175909.
Tømmervik, H., Dunfjeld, S., Olsson, G.A., Nilsen, M.Ø., 2010. Detection of ancient reindeer pens, cultural remains and anthropogenic influenced vegetation in Byrkije (Børgefjell) mountains, Fennoscandia. Landsc. Urban Plan. 98, 56–71. https://doi.org/10.1016/j.landurbplan.2010.07.010.
Walker, D.A., Raynolds, M.K., Daniëls, F.J.A., Einarsson, E., Elvebakk, A., Gould, W.A., et al., 2005. The circumpolar Arctic vegetation map. J. Veg. Sci. 16, 267–282. https://doi.org/10.1111/j.1654-1103.2005.tb02365.x.
Weijers, S., Buchwal, A., Blok, D., Löffler, J., Elberling, B., 2017. High Arctic summer warming tracked by increased Cassiope tetragona growth in the world's northernmost polar desert. Glob. Chang. Biol. 23, 5006–5020. https://doi.org/10.1111/gcb.13747.
Wolfe, S.A., Nickling, W.G., 1993. The protective role of sparse vegetation in wind erosion. Prog. Phys. Geogr. Earth Environ. 17, 50–68. https://doi.org/10.1177/030913339301700104.

Web sources

The national database of cultural heritage monuments and properties (Nunniffiit), r. http://nunniffiit.natmus.gl (Last visited August 2018).